

See discussions, stats, and author profiles for this publication at: <https://www.researchgate.net/publication/40896959>

Canonical and microcanonical analysis of nongrafted homopolymer adsorption by an attractive substrate

ARTICLE *in* THE JOURNAL OF CHEMICAL PHYSICS · DECEMBER 2009

Impact Factor: 2.95 · DOI: 10.1063/1.3273418 · Source: PubMed

CITATIONS

12

READS

35

5 AUTHORS, INCLUDING:



Lei Wang

University of Science and Technology of China

10 PUBLICATIONS 71 CITATIONS

SEE PROFILE



Yuan Liu

University of Science and Technology of China

12 PUBLICATIONS 222 CITATIONS

SEE PROFILE



Haojun Liang

University of Science and Technology of China

152 PUBLICATIONS 2,247 CITATIONS

SEE PROFILE

Canonical and microcanonical analysis of nongrafted homopolymer adsorption by an attractive substrate

Lei Wang, Tao Chen, Xiangsong Lin, Yuan Liu, and Haojun Liang^{a)}

Department of Polymer Science and Engineering, CAS Key Laboratory of Soft Matter Chemistry, Hefei National Laboratory for Physical Sciences at Microscale, University of Science and Technology of China, Hefei, Anhui 230026, People's Republic of China

(Received 27 July 2009; accepted 18 November 2009; published online 28 December 2009)

Using the off-lattice Monte Carlo simulation and replica-exchange method, we studied the behavior of nongrafted homopolymer adsorption by an attractive substrate from both the canonical and the microcanonical views. An adsorption transition is identified from the peak in canonical specific heat and compared with the conventional polymer adsorption with one end anchored on the surface of the substrate. Judging from the typical “backbending effect” and the negative specific heat in microcanonical ensemble, the transition is first-order-like when adsorption is relatively strong. However, it becomes second-order-like when the strength of adsorption becomes weak enough. Further study reveals that for a chain consisting of a limited number of monomers, the type of this transition becoming either first- or second-order-like depends not only on the interplay between monomer-monomer and monomer-substrate interaction, but also on the width of the gap in which it is confined. © 2009 American Institute of Physics. [doi:10.1063/1.3273418]

I. INTRODUCTION

Conformational behavior of homopolymers or heteropolymers near substrates has been widely studied during the past decades using scaling theory,^{1,2} mean-field density functional theory,^{3,4} and many other methods.^{5–11} Inspired by subjects such as the stability of colloidal suspensions³ and the behaviors of biological molecules,^{12,13} these studies are of essential biological and technological significance.

From the biological point of view in particular, experiments such as peptide binding to metal or semiconductor surfaces^{12,13} attracted increasing attention especially in models of nongrafted polymer adsorption (NPA). Typically, most studies concerning polymer behavior near a substrate have been performed using the model of the polymer with one end explicitly anchored on the surface,^{5–10} while transition between the “adsorbed phase” and the “freely moving phase” which could happen only in nongrafted cases, has hardly been considered until recently. Bachmann and Janke^{11,14} described in detail the temperature and solubility dependence of adsorption properties for 100-mer and 200-mer homopolymers which are not fixed at the surface of the substrate. Chen *et al.*¹⁵ observed a first-order-like transition in the adsorption of a nongrafted homopolymer when very short chains are considered.

Moreover, computer simulations and real experiments are limited to small systems. As has already been pointed out,^{16–19} instead of discontinuities, smooth peaks of the specific heat of small systems in the canonical ensemble (CE) can be viewed as the direct finite size counterparts of macroscopic phase transitions, although it is difficult to distinguish whether the transition is of first or second order. Furthermore, the microcanonical ensemble (MCE) has been

reported to be a very useful tool in investigating first-order-like transitions in small systems such as peptide aggregation,^{20,21} hydrophobic segment association in a heteropolymer,²² homopolymer aggregation,²³ and protein folding.²⁴ At these transitions, the microcanonical entropy $S(E)$ exhibits a convex intruder, the microcanonical inverse temperature $T^{-1}(E) = \partial S(E) / \partial E$ shows typical backbending, and the specific heat $C_V(E) = \partial E / \partial T(E) = -(\partial S / \partial E)^2 / (\partial^2 S / \partial E^2)$ is negative in the corresponding region of E , implying that the system becomes cooler as energy increases. As a result, E is a more appropriate external control parameter than T here. It must be noted that small systems are not just simplified models for macrosystems but real physical systems, and “backbending effects” observed in these systems are real physical effects that are responsible for the corresponding transitions.^{25,26}

According to Bachmann's study,^{11,14} the main difference between grafted polymer adsorption (GPA) and NPA is the occurrence of the binding-unbinding transition observed in the latter case. Chen *et al.*¹⁵ gave a microcanonical analysis of the first-order-like transition observed in the NPA of 40-mer chain and indicated that whether this transition is first- or second-order-like depends on the chain length and the interplay between monomer-monomer and monomer-substrate interaction. Focusing on systems of finite size, we will use a generalized off-lattice model to provide detailed discussion on this issue from both the canonical and the microcanonical views.

II. SIMULATION DETAILS

We perform the replica-exchange method²⁷ (REM) simulation and then use a combination of the canonical and the microcanonical analyses to study the coarse-grained model of nongrafted homopolymer adsorption by attractive sub-

^{a)}Electronic mail: hjiang@ustc.edu.cn.

strate. In this section, we will describe the model, introduce REM together with the ensemble (CE) and the MCE, and provide definition of the parameters used for analysis.

A. Model for nongrafted homopolymer adsorption

Considering homopolymer in dilute solution only, a 3D off-lattice model is used to simulate a single homopolymer consisting of N repeating monomers. Our simulations are performed with the homopolymer moving between an attractive and a neutral substrate, both of which are impenetrable and the width of the gap between them, L , is suitably chosen such that a high efficiency of sampling is guaranteed.

The total energy of our system is given by

$$E_{\text{tot}} = E_{\text{int}} + E_{\text{ads}}, \quad (1)$$

where the intrinsic energy E_{int} of the polymer chain is the summation of the Lennard-Jones potential energy between all monomer pairs,

$$E_{\text{int}} = 4\epsilon_{mm} \sum_{i=1}^{N-2} \sum_{j=i+2}^N \left(\frac{1}{r_{i,j}^{12}} - \frac{1}{r_{i,j}^6} \right), \quad (2)$$

where $r_{i,j} = |\vec{r}_j - \vec{r}_i|$ is the distance between the i th and j th monomer. As to the adsorption energy E_{ads} , we consider that the attractive substrate consists of continuous monomerlike particles, and the adsorption energy of the i th monomer is produced by integrating from $z_{i,s} = z_s - z_i$, the distance between the i th monomer and the substrate's planar surface, to infinity,

$$E_{\text{ads}} = \epsilon_{ms} \sum_{i=1}^N \left[\frac{2}{15z_{i,s}^9} - \frac{1}{3z_{i,s}} \right]. \quad (3)$$

E_{int} and E_{ads} are chosen in such a way that they are comparable. Thus, by controlling ϵ_{mm} and ϵ_{ms} (in unit of $k_B T$), we were able to build the NPA model under different environmental conditions, say, the Θ condition, under which the polymer chain behaves like an ideal chain.

B. Simulation method

In MC simulation, the most frequently used ensemble is CE, in which the system evolves while exchanging energy with a reservoir at temperature T , and the Boltzmann energy distribution of this system is given by

$$P(E; T) = \frac{g(E) \exp(-E/k_B T)}{Z(T)}, \quad (4)$$

where $g(E)$ is the number of states possessing energy E , and $Z(T) = \sum_E g(E) \exp(-E/k_B T)$ is the partition function. The CE average of any observable O can be easily retrieved from

$$\langle O \rangle = \frac{\sum_E O(E) g(E) \exp(-E/k_B T)}{Z(T)}. \quad (5)$$

Obviously, once the density of states $g(E)$ is accurately extracted, any statistical quantity can be directly calculated for all temperatures using Eq. (5). However, the energy landscape of even a small system is very complicated and has many local minima; thus, an ergodic of conformation space

seems impractical for a single canonical simulation.

To solve this problem, we used REM (Ref. 27) to obtain a precise estimate of $g(E)$. In REM, M replicas run from the initial states $X = \{X_1, \dots, X_m, X_{m+1}, \dots, X_M\}$ in CE at different temperatures $T = \{T_1 > \dots > T_{m-1} > T_m > \dots > T_M\}$ independently and simultaneously, and after certain MC steps, conformations of neighboring replicas will be exchanged, according to the transition probability,

$$\omega(X_m \leftrightarrow X_{m+1}) = \begin{cases} \exp(-\Delta) & \Delta > 0 \\ 1 & \Delta \leq 0 \end{cases}, \quad (6)$$

where $\Delta = (T_m^{-1} - T_{m+1}^{-1})(E(X_{m+1})/k_B - E(X_m)/k_B)$, and X_m and X_{m+1} are conformations of the m th and $(m+1)$ th replicas, respectively. Normal MC steps and replica-exchange step will be performed alternately for long enough, say, 10^{10} MC steps in our simulation.

After REM, $g(E)$ is obtained using multiple-histogram reweighting techniques,^{28,29} to be specific, the following WHAM equations:

$$g(E) = \frac{\sum_{m=1}^M N_m(E)}{\sum_{m=1}^M n_m \exp(f_m - E/k_B T_m)}, \quad (7)$$

where

$$\exp(-f_m) = \sum_E g(E) \exp(-E/k_B T_m), \quad (8)$$

$N_m(E)$ and n_m are the histogram and the total number of samples in the m th replica, respectively. $g(E)$ and f_m are then determined by solving Eqs. (7) and (8) iteratively. By simply using the trajectory of single REM simulation, another form of canonical expectation of observable O can be written as

$$\langle O \rangle = \frac{1}{Z(T)} \sum_{m=1}^M \sum_{X_m} \frac{O(X_m) \exp(-E(X_m)/k_B T)}{\sum_{l=1}^M n_l \exp(f_l - E(X_m)/k_B T_l)} \quad (9)$$

and

$$Z(T) = \sum_{m=1}^M \sum_{X_m} \frac{\exp(-E(X_m)/k_B T)}{\sum_{l=1}^M n_l \exp(f_l - E(X_m)/k_B T_l)}, \quad (10)$$

where \sum_{X_m} means the integral of every conformation sampled during the production run of the m th replica. By changing the order of the integration, one can also easily prove Eq. (9) equals Eq. (5) and so does $Z(T)$.

Furthermore, for a small system undergoing a first-order-like transition, there will be no strict one-to-one correspondence between temperature T and energy E in the transition region, and MCE will be more sensitive than CE.²⁴ Since CE may also be considered as composed of a series of MCE with increasing energy bins, $g(E)$ can be connected to the microcanonical entropy $S(E)$ by $S(E) = \ln g(E)$ (in unit of $k_B T$). Fortunately, after a single REM run, we can extract $g(E)$, and the energetic information of any observable, i.e., $O(E)$; thus, enabling the presentation of analysis from both the canonical and the microcanonical views.

C. Parameters used for discussion

To clearly monitor the change in conformation during polymer adsorption, perpendicular (to the surface of substrate, the same below) and parallel components of radius of gyration R_g are given by

$$R_{g,\perp}^2 = \sum_{i=1}^N \left(z_i - \frac{1}{N} \sum_{i=1}^N z_i \right)^2 \quad (11)$$

and

$$2R_{g,\parallel}^2 = \sum_{i=1}^N \left(x_i - \frac{1}{N} \sum_{i=1}^N x_i \right)^2 + \sum_{i=1}^N \left(y_i - \frac{1}{N} \sum_{i=1}^N y_i \right)^2, \quad (12)$$

where coefficient 2 multiplied here for $R_{g,\parallel}$ weighs $R_{g,\perp}$, satisfying $R_g^2 = R_{g,\perp}^2 + 2R_{g,\parallel}^2$.

Another geometrical quantity used for describing NPA and GPA is the distance of polymer chain's center of mass from the surface of substrate, which reads as

$$D_z = \left| z_s - \frac{1}{N} \sum_{i=1}^N z_i \right|. \quad (13)$$

From Eq. (3), the lowest value of E_{ads} will be approximately $-1.054N\epsilon_{ms}$ considering the polymer chain adsorbed by the substrate with $z_{i,s} = (0.4)^{1/6}$ for all monomers, and the effective number of monomers adsorbed can then be defined as

$$N_{\text{ads}}^{\text{eff}} = \frac{E_{\text{ads}}}{-1.054\epsilon_{ms}}. \quad (14)$$

For the canonical analysis, specific heat capacity

$$C_V = \frac{d\langle E \rangle}{dT} = \frac{\langle E^2 \rangle - \langle E \rangle^2}{k_B T^2} \quad (15)$$

is introduced to give fluctuation of $\langle E \rangle$ versus the external control parameter T . As to the microcanonical part, two main definitions are the microcanonical inverse temperature $T^{-1}(E)$ and the loss of entropy $\Delta S(E)$, which will be given at the first stage of the discussion when MCE is taken into account.

III. RESULTS AND DISCUSSIONS

A. First-order-like transition in adsorption of nongrafted polymer

In this section, we use our designed model to make a comparison between NPA and GPA mentioned above. For the sake of generalization, simulation of a real chain case will be performed by giving the same set of nonzero parameters to both models. Considering that under certain L , it is the ratio of $\epsilon_{ms}/\epsilon_{mm}$ that determines the nature of adsorption, $\epsilon_{mm}=1.0$ is fixed and only ϵ_{ms} is adjustable. First, a polymer chain of 40 monomers with an arbitrarily chosen $\epsilon_{ms}=5.0$ representing relatively strong adsorption is taken into account ($L=4N$ is fixed to simplify discussion in this part, while a further investigation on the effect of finite L will be given in the next section).

From the point of view of CE, fluctuation of thermodynamic quantities as a function of temperature is always used

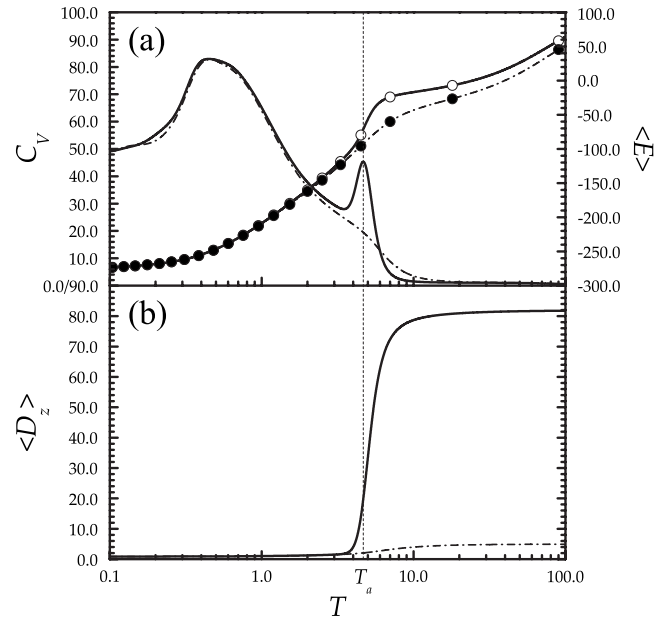


FIG. 1. (a) Canonical mean energy $\langle E \rangle$, specific heat C_V , and (b) $\langle D_z \rangle$ of NPA (solid line) and GPA (dash-dotted line) for polymer of 40 monomers, given the same parameters $\epsilon_{mm}=1.0$ and $\epsilon_{ms}=5.0$. (Open and solid circles represent direct result after REM for NPA and GPA, respectively.)

to indicate phase transition in the thermodynamic limit if there is any finite discontinuity or divergence at some critical temperature. However, it is not the case in systems of finite size. It is a widely known fact^{16–19} that instead of discontinuities, smooth peaks of specific heat (or other quantities well defined) of small systems can be viewed as direct finite size counterparts of macroscopic phase transitions.

As shown in Fig. 1, $\langle E \rangle$ directly from REM [circles in Fig. 1(a)] is identical to the results calculated using Eq. (9) [lines in Fig. 1(a)], proving $g(E)$ is accurately extracted. As a monotonic function of T , $\langle E \rangle$ behaves without any obvious difference between NPA and GPA below $T=1.0$. This is because for both cases the chain is adsorbed by the substrate at lower temperatures and any energetic information will be the same except for the translational entropy. On the other hand, in the region of higher temperatures, the situation changes dramatically. The main difference of mean energy $\langle E \rangle$ and specific heat C_V between NPA and GPA is that $\langle E \rangle$ of NPA exhibits a much more rapid increase than GPA in $4.0 < T < 10.0$ with a subsequent decrease, resulting in a peak at $T_a \approx 4.68$ in C_V . Although peaks found at lower temperatures (a detailed discussion will be given in Sec. III B) appear to

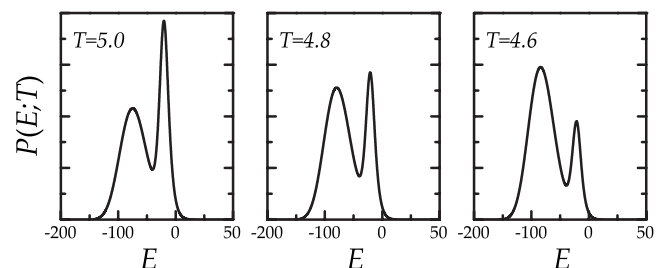


FIG. 2. Energy distribution of arbitrarily chosen temperatures in the vicinity of $T_a \approx 4.68$, $P(E;T)$ of which are all normalized (NPA with $\epsilon_{mm}=1.0$ and $\epsilon_{ms}=5.0$).

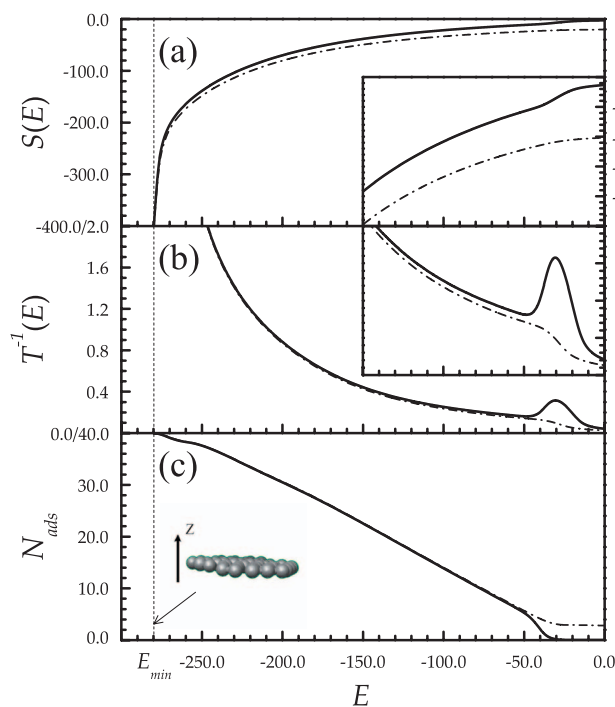


FIG. 3. (a) Microcanonical entropy $S(E)$ [for both cases $S(E_{\min})$ are set to be of the same value], (b) its derivative $T^{-1}(E) = \partial S(E) / \partial E$, namely, the microcanonical inverse temperature, and (c) $N_{\text{ads}}^{\text{eff}}$ of NPA (solid line) and GPA (dash-dotted line) with $\epsilon_{\text{mm}} = 1.0$ and $\epsilon_{\text{ms}} = 5.0$.

be more pronounced, $\langle D_z \rangle$ approaching 0.0 [Fig. 1(b)] indicates that they are the conformational transitions of the “totally adsorbed” chain, which cannot distinguish NPA and GPA. For NPA, $\langle D_z \rangle$ then exhibits an obvious jump as the temperature increases in $4.0 < T < 10.0$ and reaches 80.0 (half the distance between substrates) at higher temperatures, which means the polymer is moving freely in the whole

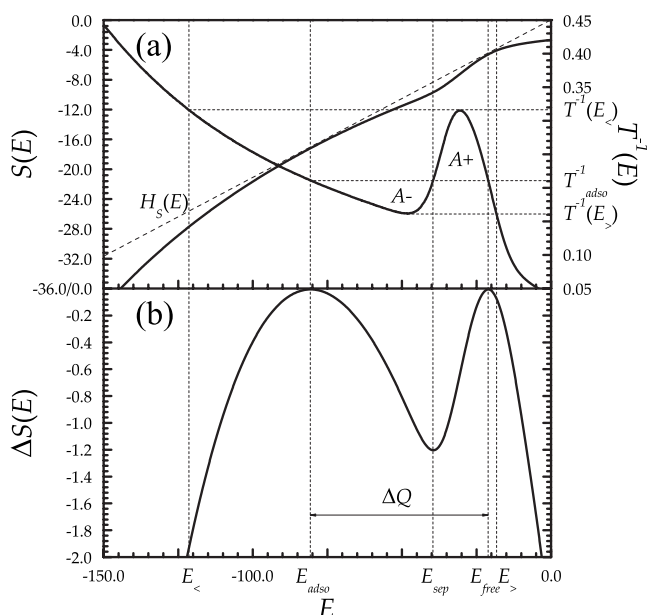


FIG. 4. Microcanonical analysis for NPA with $\epsilon_{\text{mm}} = 1.0$ and $\epsilon_{\text{ms}} = 5.0$. (a) The microcanonical entropy $S(E)$ (left scale) and the microcanonical inverse temperature $T^{-1}(E) = \partial S(E) / \partial E$ (right scale). (b) The loss of entropy $\Delta S(E) = S(E) - H_S(E)$.

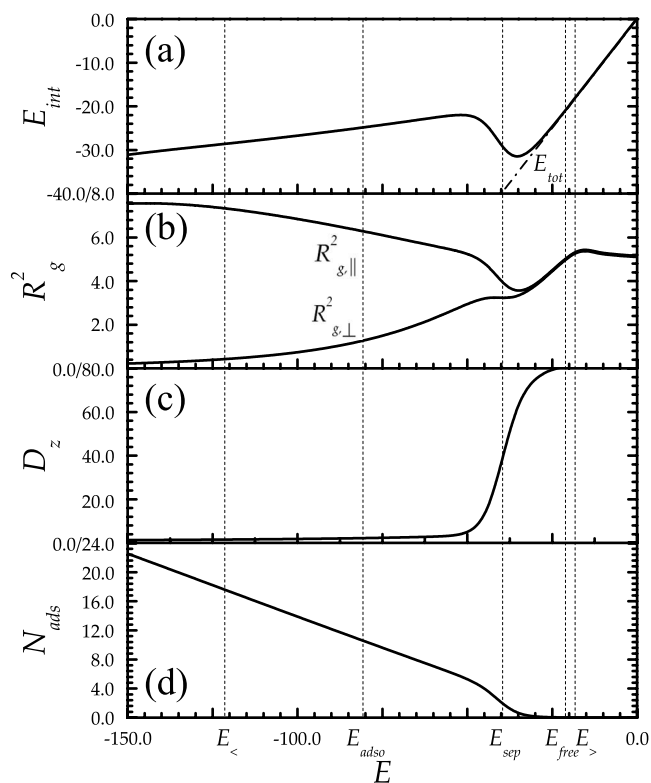


FIG. 5. (a) E_{int} , (b) R_g ($R_{g,\perp}$ and $R_{g,\parallel}$), (c) D_z , and (d) $N_{\text{ads}}^{\text{eff}}$ at the transition region (NPA with $\epsilon_{\text{mm}} = 1.0$ and $\epsilon_{\text{ms}} = 5.0$).

space. This transition is shown to be from the “adsorbed phase” to the “freely moving phase” driven by temperature, which coincides with the observations of Bachmann and Janke.¹¹ However, with peaks of specific heat in CE, we cannot draw any conclusion about the nature of this transition. Energy distributions in the vicinity of transition temperature T_a are plotted in Fig. 2. The bimodal energy distribution shows that transition in NPA is first-order-like. It

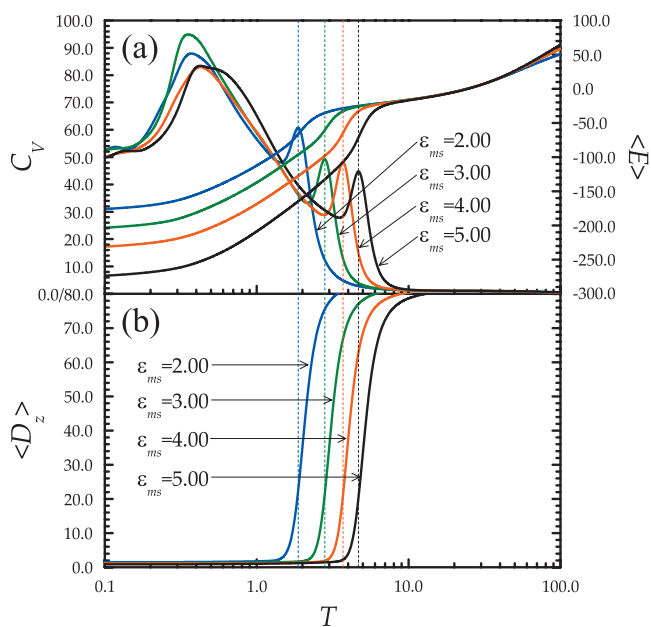


FIG. 6. (a) Canonical mean energy $\langle E \rangle$, specific heat C_V , and (b) $\langle D_z \rangle$ of different value of ϵ_{ms} with $\epsilon_{\text{mm}} = 1.00$ fixed for NPA of a 40-mer chain.

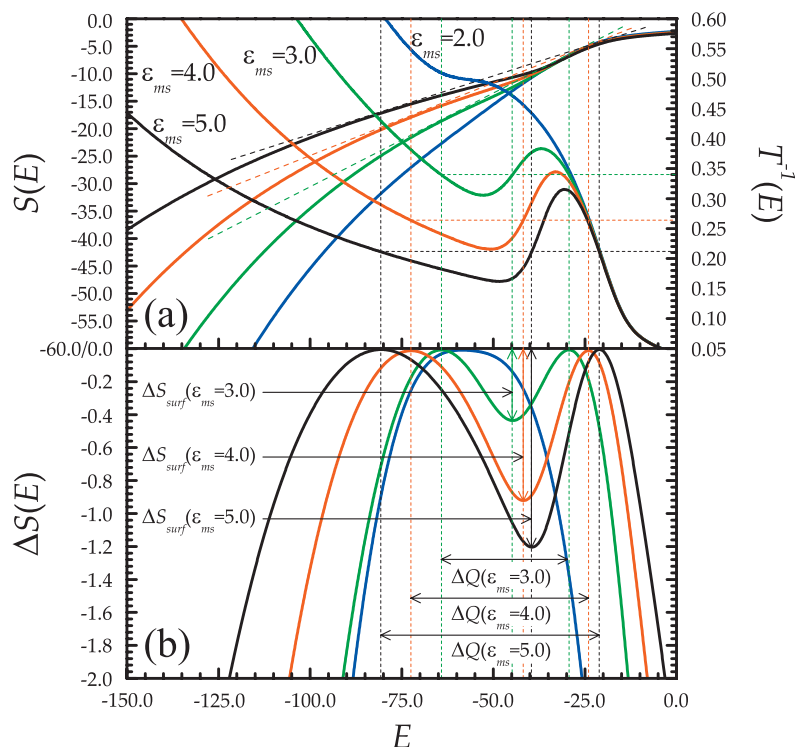


FIG. 7. (a) Microcanonical entropy $S(E)$ (left scale), inverse temperature $T^{-1}(E)$ (right scale), and (b) loss of entropy $\Delta S(E)$ of different values of ϵ_{ms} with $\epsilon_{mm} = 1.00$ fixed for NPA of a 40-mer chain.

should be pointed out that this “coexistence” of two phases is a dynamic equilibrium, as only one phase exists at any time due to the finite size of the system. The exact relationship between E and T is not clear from canonical analysis only because T as an external control parameter gives a smeared curve of E . We will now move to MCE for a more detailed analysis.

As mentioned before, MCE will be more sensitive to first-order-like transition in small systems. The microcanonical entropy $S(E)$ and its derivative $T^{-1}(E) = \partial S(E) / \partial E$ versus energy E are given in Fig. 3 for NPA and GPA respectively. The lowest energies found in NPA and GPA are of the same value, $E_{\min} = E_{\min, \text{int}} + E_{\min, \text{ads}} \approx -279.86$ with $N_{\text{ads}}^{\text{eff}} = E_{\min, \text{ads}} / (-1.054 \epsilon_{ms}) \approx 40.0$ [Fig. 3(c)], thus implying that all monomers are adsorbed at states of the lowest energy for both cases [see snapshot in Fig. 3(c)]. Due to the reduction in DOFs, $S(E)$ of GPA is comparably smaller than that of NPA for all energy bins. More importantly, the convex of $S(E)$ in NPA [inset of Fig. 3(a)] leads to an S-shaped backbending around $0.16 < T^{-1}(E) < 0.32$ [inset of Fig. 3(b)], which is in agreement with the CE result ($T_a^{-1} \approx 0.21$).

From the canonical and the microcanonical analyses, we identify that the transition of NPA that happens at T_a can be addressed as an adsorption transition between “adsorbed phase” and “freely moving phase.” Quantities with subscript “ads” and “free” will be used to represent these two phases, respectively.

We will look into this issue with more detail. In systems of finite size such as the NPA considered here, the microcanonical entropy loss together with the consequent “backbending effect” will be an important indicator for essential structural transitions.^{20–24} As shown in Fig. 4(a), the concave Gibbs hull $H_S(E) = S(E_{\text{ads}}) + E/T_{\text{ads}}$ is the tangent connecting $S(E_{\text{ads}})$ and $S(E_{\text{free}})$, the slope of which is $T_{\text{ads}}^{-1} \approx 0.21$.

The loss of entropy can then be constructed as $\Delta S(E) = S(E) - H_S(E)$ [Fig. 4(b)]. From another point of view, $P(E; T_{\text{ads}})$ is proportional to $\exp(\Delta S(E))$; to be more specific, canonical energy distribution at T_{ads} shows two peaks of equal height, which means two phases coexist at this temperature with latent heat $\Delta Q = E_{\text{free}} - E_{\text{ads}} = T_{\text{ads}}(S(E_{\text{free}}) - S(E_{\text{ads}})) \approx 59.64$. The loss of entropy further leads to the S-shaped curve [Fig. 4(a)] of microcanonical inverse temperature $T^{-1}(E) = \partial S(E) / \partial E$ in the interval $E_{<} \leq E \leq E_{>}$ or $T(E_{<}) \leq T(E) \leq T(E_{>})$, in which T and E have no strict one-to-one correspondence. The Maxwell line T_{ads}^{-1} splits the S-shaped $T^{-1}(E)$ curve into $A_+ = S(E_{\text{free}}) - S(E_{\text{sep}}) - T_{\text{ads}}^{-1}(E_{\text{free}} - E_{\text{sep}})$ and $A_- = T_{\text{ads}}^{-1}(E_{\text{sep}} - E_{\text{ads}}) - S(E_{\text{sep}}) - S(E_{\text{ads}})$. The interfacial entropy due to the boundary between two phases is $\Delta S_{\text{surf}} = A_+ = A_- = -\Delta S(E_{\text{sep}})$.³⁰

Due to the “backbending effect,” MCE gives much more pronounced signals in the regime of this first-order-like transition. To unveil its physical origin, E_{int} , R_g , D_z , and $N_{\text{ads}}^{\text{eff}}$ are plotted in Fig. 5 as functions of E at this transition. In the region $E > E_{>}$, $E_{\text{int}} \approx E_{\text{tot}}$ and $D_z \approx 80.0$ give evidence that the polymer chain is free from the substrate because the thermal energy dominates. As expected, the polymer chain changes from being isotropical in solution ($R_{g, \perp}$ and $R_{g, \parallel}$ are almost the same) to having a pancake-type geometrical 3D structure (increasing $R_{g, \perp}$ and decreasing $R_{g, \parallel}$) near the substrate’s surface as E decreases in $E_{<} \leq E \leq E_{>}$. In particular, a sudden change in structure is identified in the vicinity of E_{sep} , as $N_{\text{ads}}^{\text{eff}}$ becomes nonzero and increases, E_{int} and R_g also increase from the minimum at $E \approx -35.0$ to the maximum at $E \approx -50.0$ (where T increases as E decreases), implying a swelling “pancake” with energy not minimized. Unfavorable states at around E_{sep} try to avoid themselves and move to stable states, thus rearranging the structure and converting part of the kinetic (potential) energy into potential (kinetic)

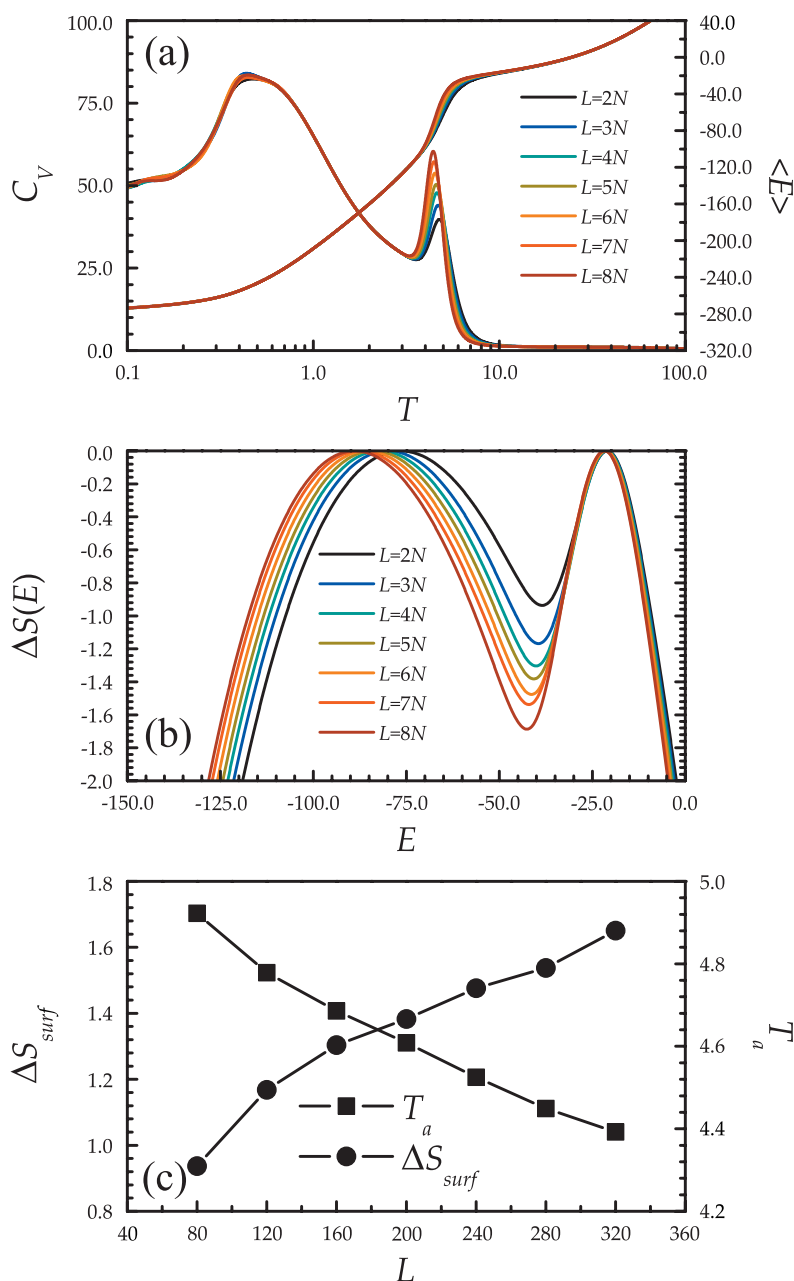


FIG. 8. (a) Canonical mean energy $\langle E \rangle$ (right scale), specific heat C_V (left scale), (b) loss of entropy $\Delta S(E)$, (c) ΔS_{surf} and T_a of different values of L with $\epsilon_{ms} = 5.00$, $\epsilon_{mm} = 1.00$ fixed for NPA of a 40-mer chain.

energy. Therefore, the system becomes warmer (colder) while E_{tot} decreases (increases), and the specific heat capacity $C_V(E) = \partial E / \partial T(E) = -(\partial S / \partial E)^2 / (\partial^2 S / \partial E^2)$ is negative correspondingly. Due to this effect our system resembles that of melting clusters²⁶ and astronomical objects.²⁵ On the other hand, for a large system undergoing a first order transition, say, solid-liquid transition, it converts energy absorbed completely into potential energy for melting continuously, and “backbending effect” and negative specific heat cannot be observed. It should be noted that these effects are due to the finite size of the system considered, and are indicators for first-order-like transitions in small systems. Judging from $D_z \approx 0.0$ in $E < E_c$, the polymer chain is adsorbed by the substrate and only the “adsorbed phase” exists.

For comparison, we also performed weaker adsorption cases by giving, say, $\epsilon_{ms} = 4.0$, 3.0, and 2.0 (all under the condition $L = 4N$). As shown in Fig. 6(a), curves of $\langle E \rangle$ and C_V exhibit a similar behavior analogous to that of $\epsilon_{ms} = 5.0$,

and adsorption transitions are found at $T_a \approx 3.70$, 2.80, and 1.87, respectively [also indicated by a sharp drop in $\langle D_z \rangle$ in Fig. 6(b)], which are lower than that of the strong adsorption case and decreasing with ϵ_{ms} .

Furthermore, phase coexistence and “backbending effect” are found at those transitions, except for when $\epsilon_{ms} = 2.0$ [Fig. 7(a)]. As shown in Fig. 7(b), ΔS_{surf} and the latent heat ΔQ are getting smaller as ϵ_{ms} decreases, which means the strength of the interfacial barrier between two phases is getting weaker. Although the peak of C_V in weak adsorption for NPA given $\epsilon_{ms} = 2.0$ is remarkable, this transition shows no “backbending effect.” Thus, no phase coexistence will be observed at the region of transition and the adsorption transition becomes second-order-like.

As to the reason, it is due to that the sudden change in the $S(E)$ of chain from “freely moving phase” to “adsorbed phase” becomes less prominent as ϵ_{ms} decreases. On one hand, $S(E)$ of freely moving phase has little change when

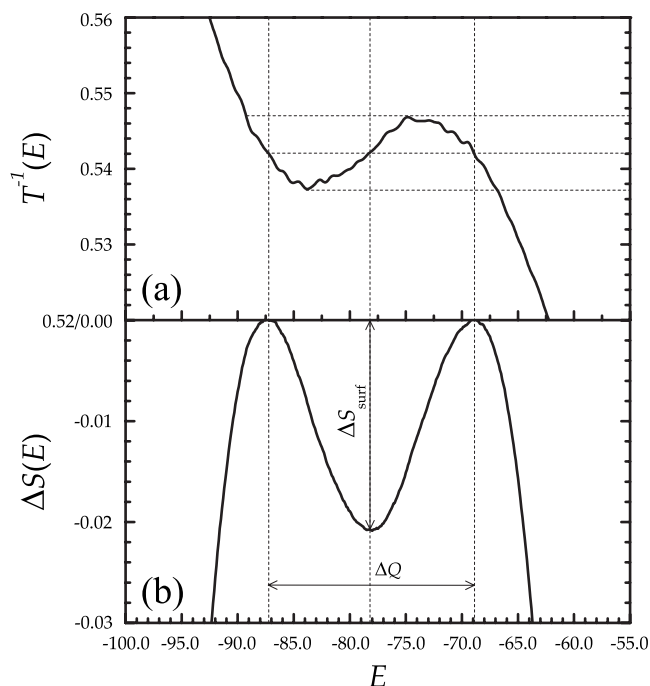


FIG. 9. (a) $T^{-1}(E)$ and (b) $\Delta S(E)$ of $L=8N$ for NPA of a 40-mer chain with $\epsilon_{ms}=2.00$, $\epsilon_{mm}=1.00$.

$L=4N$ remains the same, while on the other hand, $S(E)$ of adsorbed phase will increase because conformation of adsorbed chain will change from compact single layer or double layer to compact 3D structure as decreasing strength of adsorption.¹¹ In other words, the height of right-hand bump in plot of $S(E)$ decreases with decreasing ϵ_{ms} , resulting in decreasing ΔS_{surf} and making the transition be less first-order-like. In addition, T_a is shifting toward the peak at $T \approx 0.4$, which has been addressed to be an overlapping peak of liquid-solid-like transition and coil-to-globule transition.^{31–33} Without significant change in $S(E)$, backbending effect and negative specific heat cannot be observed; it is a second-order-like transition as we see in the case of $\epsilon_{ms}=2.0$. In summary, given finite N and L , the type of transition (i.e., first- or second-order-like) will depend on whether the ratio $\epsilon_{ms}/\epsilon_{mm}$ is above or under some certain value. It should be emphasized that the phenomenon discussed above can only be observed in a real chain model ($\epsilon_{mm}>0$) because in an athermal or ideal chain model ΔS_{surf} is sufficiently large that the adsorption transition will always be of first order. Chen *et al.* gave the result of athermal chain and the phase diagrams of NPA of a 40-mer chain,¹⁵ which is in agreement with our explanation.

From the above discussion, we have proven that a first-order-like transition indeed occurs for NPA when strong adsorption is taken into account. However, we have $L=4N$ fixed for all cases considered so far. In fact, not only the finite chain length N , but also the width of the gap L will affect the finite size effects observed. The finite size dependence of the transition will be discussed in the following section.

B. Finite size dependence of the transition

As mentioned previously, a neutral substrate is placed to prevent the chain from escaping, and the gap width L is

chosen for that its influence on chain conformation can be negligible ($L>N$). Nonetheless, $g(E)$ of chain in “freely moving phase” will be proportional to L and other observables will also depend on it. For consistency, we still use the parameters $\epsilon_{ms}=5.00$, $\epsilon_{mm}=1.00$, and increase L (from $2N$ to $8N$) to show effects induced by finite width of the gap (Fig. 8). It is undoubted that the number of MC steps should be linearly increasing with L , and the sampling of all possible states will become much more difficult.

As can be seen in Fig. 8(a), as L increases, $\langle E \rangle$ changes little except in the transition region, where C_V becomes sharper and sharper, indicating that the transition is more and more first-order-like. It will be much clearer from the microcanonical view. For the chain in “freely moving phase,” $S(E)$ will increase as L increases. The right-hand bumps in plots of $S(E)$ and $\Delta S(E)$ [Fig. 8(b)] then increase for the reason that the entropy of chain in “adsorbed phase” is independent of L , thus, making ΔS_{surf} also increase with L [Fig. 8(c)]. Another comprehensible effect due to the increasing L is the slight shift in T_a toward lower temperature [Fig. 8(c)], which is also induced by increasing height of the bump. Now let us reconsider the case $\epsilon_{ms}=2.00$ and increase L to $8N$. In Fig. 9, the typical backbending in $T^{-1}(E)$ and $\Delta S_{\text{surf}} \approx 0.021$ clearly illustrated that the transition becomes first-order-like as expected, compared to the result of $L=4N$ (Fig. 7). This phenomenon is very interesting since the nature of the transition changes with the width of the gap in which the polymer is confined. It can be concluded that for any case with different $\epsilon_{ms}/\epsilon_{mm}$, the adsorption will be first-order-like for sufficiently large L . To summarize, there is an L -dependence in the adsorption transition of NPA.

As to the N -dependence, it has already been proven that NPA of 10-mer homopolymer is first-order-like while 80-mer case (with the same ϵ_{mm} and ϵ_{ms}) shows a second-order-like feature.¹⁵ However, this conclusion is definitely right only when L has been fixed for all cases compared. In other words, we cannot easily extrapolate any conclusion to systems of larger N without considering L -dependence. These effects together with the long computational time required to obtain the $g(E)$ of NPA of very long chains makes the investigation of N -dependence a much more complicated and delicate issue. Other methods and analysis may thus be introduced to provide an integrated explanation to this question.

Although the L - and N -dependences of the transition are of great interest, the NPA considered here is a small system of which finite size effects are the main reason for the backbending effect. It should be noted further that, inspired by experiments,^{12,13} the NPA of short chain is a generalized model that reflects the real physical phenomenon of polymer with a very limited number of segments.

IV. CONCLUSION

Using a combination of the canonical and the microcanonical analyses, we identified that a phase transition indeed occurs in the adsorption of nongrafted homopolymer consisting of a limited number of monomers, which cannot be observed in adsorption of homopolymer with one of its end explicitly anchored on the substrate. Furthermore, transition

is first-order-like and typical backbending effect is observed in the microcanonical analysis when strong adsorption case is performed, while it becomes second-order-like without such effect in correspondingly weak adsorption. However, as L increases, the adsorption transition becomes more and more first-order-like. In summary, the type of the transition becoming either first- or second-order-like depends not only on $\epsilon_{ms}/\epsilon_{mm}$ and N , but also on L . In other words, there is an L -dependence in the adsorption transition of nongrafted polymer of very finite length.

ACKNOWLEDGMENTS

We are grateful for the financial support provided by the Outstanding Youth Fund (Grant No. 20525416), Program of the National Natural Science Foundation of China (Grant Nos. 20874094, 50773072, and 20934004), and NBRPC (Grant No. 2005CB623800). Simulations were carried out at the Shanghai Supercomputer Center.

¹P. G. De Gennes, *Scaling Concepts in Polymer Physics* (Cornell University Press, Ithaca, 1979).

²E. Eisenriegler, K. Kremer, and K. Binder, *J. Chem. Phys.* **77**, 6296 (1982).

³J. Forsman and C. E. Woodward, *Phys. Rev. Lett.* **94**, 118301 (2005).

⁴E. Eisenriegler, *Polymer Near Surfaces* (World Scientific, Singapore, 1993).

⁵R. Hegger and P. Grassberger, *J. Phys. A* **27**, 4069 (1994).

⁶T. Vrbová and K. Procházka, *J. Phys. A* **32**, 5469 (1999).

⁷Y. Singh, D. Giri, and S. Kumar, *J. Phys. A* **34**, L67 (2001).

⁸M. S. Causo, *J. Chem. Phys.* **117**, 6789 (2002).

⁹F. Celestini, T. Frisch, and X. Oyharzabal, *Phys. Rev. E* **70**, 012801

(2004).

¹⁰P. Benetatos and E. Frey, *Phys. Rev. E* **70**, 051806 (2004).

¹¹M. Bachmann and W. Janke, *Phys. Rev. Lett.* **95**, 058102 (2005).

¹²S. R. Whaley, D. S. English, E. L. Hu, P. F. Barbara, and A. M. Belcher, *Nature (London)* **405**, 665 (2000).

¹³K. Goede, P. Busch, and M. Grundmann, *Nano Lett.* **4**, 2115 (2004).

¹⁴M. Bachmann and W. Janke, *Phys. Rev. E* **73**, 041802 (2006).

¹⁵T. Chen, L. Wang, X. S. Lin, Y. Liu, and H. J. Liang, *J. Chem. Phys.* **130**, 244905 (2009).

¹⁶K. Binder, *Rep. Prog. Phys.* **50**, 783 (1987).

¹⁷P. Labastie and R. L. Whetten, *Phys. Rev. Lett.* **65**, 1567 (1990).

¹⁸P. Borrmann, O. Mülken, and J. Harting, *Phys. Rev. Lett.* **84**, 3511 (2000).

¹⁹J. Dunkel and S. Hilbert, *Physica A* **370**, 390 (2006).

²⁰C. Junghans, M. Bachmann, and W. Janke, *Phys. Rev. Lett.* **97**, 218103 (2006).

²¹C. Junghans, M. Bachmann, and W. Janke, *J. Chem. Phys.* **128**, 085103 (2008).

²²T. Chen, X. S. Lin, Y. Liu, and H. J. Liang, *Phys. Rev. E* **76**, 046110 (2007).

²³T. Chen, X. S. Lin, Y. Liu, and H. J. Liang, *Phys. Rev. E* **78**, 056101 (2008).

²⁴J. Hernández-Rojas and J. M. Gomez-Llorente, *Phys. Rev. Lett.* **100**, 258104 (2008).

²⁵W. Thirring, *Z. Phys.* **235**, 339 (1970).

²⁶M. Schmidt, R. Kusche, T. Hippler, J. Donges, W. Kronmüller, B. von Issendorff, and H. Haberland, *Phys. Rev. Lett.* **86**, 1191 (2001).

²⁷A. Mitsutake, Y. Sugita, and Y. Okamoto, *J. Chem. Phys.* **118**, 6664 (2003).

²⁸A. M. Ferrenberg and R. H. Swendsen, *Phys. Rev. Lett.* **63**, 1195 (1989).

²⁹S. Kumar, D. Bouzida, R. H. Swendsen, P. A. Kollman, and J. M. Rosenberg, *J. Comput. Chem.* **13**, 1011 (1992).

³⁰W. Janke, *Nucl. Phys. B, Proc. Suppl.* **63A-C**, 631 (1998).

³¹Y. Zhou, C. K. Hill, and M. Karplus, *Phys. Rev. Lett.* **77**, 2822 (1996).

³²H. J. Liang and H. N. Chen, *J. Chem. Phys.* **113**, 4469 (2000).

³³F. Rampf, W. Paul, and K. Binder, *Europhys. Lett.* **70**, 628 (2005).